Postprint. Jing Deng, et al., Industrial & Engineering Chemistry Research 2020, 59, 32, 14458–14466.
https://doi.org/10.1021/acs.iecr.0c01946

Effects of the Morphology of the ZIF on the CO_2 Separation Performance of MMMs

Jing Deng[a,c]†, *Zhongde Dai*[b,c]† *and Liyuan Deng*[a,]*

[a]: Department of Chemical Engineering, Norwegian University of Science and Technology, 7491 Trondheim, Norway

[b]: College of Architecture & Environment, Sichuan University, 610065 Chengdu, China

[c]: School of Chemical, Biological and Material Engineering, University of Oklahoma, Norman, Oklahoma, Unite State

† These authors contributed equally.

KEYWORDS:

Mixed matrix membranes; effects of filler morphology; ZIFs, Pebax 2533; CO_2/N_2 separation.

ABSTRACT

In this study, three zeolitic imidazolate frameworks (ZIFs) with different shapes – particles (0D), microneedles (1D) and leaves (2D) - were synthesized by tuning the polymeric additive. These ZIFs have been dispersed into Pebax 2533 matrix with a loading varying from 0 to 20 wt.%. The resultant mixed matrix membranes (MMMs) have been systemically characterized by various techniques. Mixed gas permeation experiment was also employed to evaluate the CO_2 separation performance. The results show that there exists an optimal ZIF loading for these three series of membranes, but the values are highly dependent on the morphologies of the added ZIFs. The membranes containing ZIF particles and microneedles display the highest CO_2 permeability and CO_2/N_2 selectivity simultaneously at 10 wt.% loading, while a much lower loading, i.e., ~ 5 wt.% is the optimized value for ZIF leaves. Moreover, the increment in CO_2 permeability is related to the ZIFs' morphology and the order is 0D < 1D < 2D. On the other hand, the effects of the morphology on selectivity seems to be the opposite, with ZIF of 0D structure showing the highest selectivity. Moreover, the influences of adding ZIF fillers on the performances of the resultant MMMs under varied operating temperatures and the feed pressures were also investigated. The membrane with 10 wt.% 1D ZIF shows the highest increment in CO_2 permeability (727.4 Barrer) with the CO_2/N_2 selectivity of ~ 14 at 60 ^oC.

1. Introduction

The market size of gas separation membranes in various applications, like air separations and natural gas sweetening/dehydration, has been expanding greatly [1-5] and is estimated to reach $1.1 billion by 2024 according to a very recent research report.[6] Among plenty of the membrane materials, polymers have dominated due to their low cost, excellent processability and easy scale-up. But in most fields, especially for CO_2 separation, one of the biggest markets, the current polymeric membrane materials still cannot meet the desirable performance to replace the conventional separation technology (e.g., absorption/adsorption), which usually are energy-intensive processes. The present polymeric materials either have high gas permeabilities with low gas selectivity, or vice versa, known as the "Upper Bound".[7]

On the other hand, the inorganic membrane materials usually have high gas transport properties and selectivity at the same time. However, their high cost and poor processability hinder them from gaining wide application. Hence, an alternative that potentially combines the benefits and avoids the disadvantages of both polymeric and inorganic membranes, known as mixed matrix membranes (MMMs),[4, 8-10] has been proposed by incorporating inorganic fillers into polymeric matrix. Generally speaking, the incorporation of inorganic fillers could have a positive effect in the gas diffusivity. Song et al. has blended ZIF-8 (zeolitic imidazolate framework) nanoparticles into Matrimid and observed a monotonous increment in gas permeability with increasing ZIF-8 content.[11] Further analysis suggests that the enhanced CO_2 permeability is mainly due to the increased CO_2 diffusivity, which comes from the higher free volume created by the rigidified polymeric matrix due to the presence of the ZIF-8, as well as the extra transport path inside ZIF-8 particles. Moreover, the angstrom-scale pores or special channels inside the ZIF fillers offer not

only extra transport paths, but also work as a molecular sieve and thus promote the separation performance. Another research documented that the interlayer channels inside graphene oxide could work as fast and selective pathways for CO_2, and only 1 wt.% graphene oxide could realize significant increments in both CO_2 permeability and CO_2/N_2 selectivity, thereby surpassing the "Upper Bound".[12] In addition, the rich diversity in the polymer-inorganic filler pairs offers great probability of achieving better membranes.

Despite these encouraging results, there still exists lots of problem that are yet not to be fully understood. Researchers have noticed that incorporating inorganic nano-fillers into polymeric matrix could also result in deteriorated performance. Various factors, such as fillers' pore size / shapes, the size / shape / chemical composition of the fillers, the pairing selection of fillers and polymeric matrix, preparation methods, could affect the morphology of the resultant MMMs and thus the performances. Very recently, it has been reported that the altering filler's geometry may result in different performances, even with the same pairing (polymer-fillers). [13] For instance, several studies have found that increasing filler size has negative effects on the gas permeabilities [14-16] with the same loading, since the smaller fillers could offer more external surface area. On the other hand, larger particles have less tendency to form agglomeration and may benefit the gas transport properties of the resultant membranes. [15, 17, 18]

Apart from the size effect, the filler shape is also considered as one of crucial factors, which would affect greatly the interfacial contact between fillers and the polymeric matrix. However, only a few related researches have been conducted. Sabetghadam and co-workers [19] prepared NH_2-MIL-53(Al)s nanoparticles (46 × 15 nm), nanorods (64 × 15 nm) and microneedles (4000 × 80 nm) by different preparation methods and incorporated them into Matrimid to investigate the effect of MOF's morphology on the performance of the resultant MMMs. The gas permeation results show

that the nanoparticles could benefit the gas permeability, while the addition of the other MOFs leads to a loss in CO_2 permeability. The better dispersion of nanoparticles inside polymeric matrix is believed to be the main reason, since the nanorods and microneedles have higher aspect ratio and thus less closer to the ideal sphere. The same group also demonstrated that the presence of copper 1,4-benzenedicarboxylate (CuBDC) nanosheets in Matrimid matrix increases the CO_2/CH_4 selectivity while the nanoparticles or bulk-type analogies worsen the separation ability of the polymeric matrix.[20]

In another work by our group, a simple method to prepare ZIF cuboids with different thicknesses has been reported. These ZIFs were then incorporated into Pebax matrix for gas separation. Results show the ZIFs with different thicknesses could result in considerably distinct impacts on the CO_2 separation performance: the thickest one brings about the highest CO_2 permeability.[21] In the current work, following the same ideas, the influences of the filler shapes on the properties of the ZIF + Pebax matrix were investigated by employing ZIF nanoparticles (0D), needles (1D) and leaves (2D). These ZIFs were prepared using different methods at room temperature, and then analyzed by various characterization techniques: scanning electron microscope (SEM), fourier-transform infrared (FTIR) spectroscopy and X-ray crystallography (XRD). Afterwards, these methods were also used to evaluate the properties of the resultant MMMs together with thermal analysis (TGA) and differential scanning calorimetry (DSC). Finally, the CO_2/N_2 separation performance was studied by mixed gas permeation tests and the correspondence between the morphologically properties of the nanofillers and the permeation properties of the MMMs are discussed.

2. Experimental Section

2.1. Materials

$Zn(NO_3)_2 \cdot 6H_2O$, 2-methylimidazole (Hmim), Poly(vinyl alcohol) (PVA, M_n 89000-98000 g/mol, 99% hydrolyzed) and polyethylene glycol (400g/mol, PEG 400) were ordered from Sigma, Norway. Pebax 2533 pellets were purchased from Arkema. Ethanol (96%) was bought from VWR, Norway. All the chemicals were used without further treatment.

2.2. ZIFs preparation

The ZIFs synthesized in PEG 400, PVA and additive-free solution have a morphology of particles, microneedles and leaves, which are named as 0D ZIF, 1D ZIF and 2D ZIF, respectively. The 0D ZIF and 1D ZIF were prepared via the following procedure: 0.59g $Zn(NO_3) \cdot 6H_2O$ was dissolved in 40 mL 1 wt.% PVA or PEG solution, while 1.32 g Hmim was added into another 40 mL same polymeric solution (1 wt.%). Then two solutions were mixed and stirred at room temperatures and solution gradually became whitish. 2D ZIF was prepared according to the same procedure but in DI water. After 3 hours, the solution was centrifuged at 10000 rpm for 10 mins and then the precipitate was as-synthesized ZIFs. The obtained ZIFs were washed twice by dispersing in DI water and centrifuging to remove residual reactants and the polymeric additives. Finally, the ZIFs were placed in vacuum oven at 60 ^oC until fully dried.

2.3. Membrane preparation

Pebax 2533 + ZIFs membranes were fabricated by the knife-casting method. Typically, 8 wt.% Pebax 2533 / ethanol solution was prepared at 80 °C with reflux for around 2 hours. Meanwhile, a certain amount of ZIFs was added into ethanol to prepare the 8 wt.% ZIF / ethanol suspension. Afterwards, the Pebax solution was added into the ZIF / ethanol suspension, accompanied by stirring, overnight. The mixture was cast on a glass plate using a casting knife (PA-4302, BYK-CHEMIE GMBH, Germany) with a wet gap of around 600 μm, and, as a result, the thickness of

obtained membrane is around 30 – 40 μm. The cast membrane was then dried in a ventilated oven at 40 °C and then moved to a vacuum oven at 60 °C until fully dry. The obtained membranes were stored in a desiccator to avoid the absorption of moisture from air.

2.4. Characterization

The FTIR spectroscopy was performed for all ZIFs and resultant membranes with a Nicolet Nexus spectrometer, Thermo. The obtained spectra of all samples were an average of 16 scans with wavenumber from 550 cm^{-1} to 4000 cm^{-1}.

The morphologies of ZIFs and the resultant MMMs were analyzed using a SEM (TM3030 tabletop microscope, Hitachi). The cross-section specimens of MMMs were prepared by breaking the samples in liquid N_2. A sputter coating with gold (2 mins) was conducted for all samples before SEM characterization.

The thermal stability tests of ZIFs and the MMMs were performed by a TGA (TG 209F1 Libra, Netzsch). Samples of around 10 - 20 mg were used. All samples were heated from room temperature to 700 °C at a heating rate of 10 °C / min under N_2 atmosphere. Differential scanning calorimetry (DSC) analysis was also conducted to study the phase transition behavior of the MMMs (DSC 214 Polyma, NETZSCH-Gerätebau GmbH, Germany). Samples of around 10 - 20 mg were placed in a covered standard aluminum pan and heated at the rate of 10 °C/min in N_2 atmosphere.

The crystalline information of the as-prepared ZIFs and MMMs was obtained from XRD tests using Bruker D8 A25 DaVinci X-ray Diffractometer, Bruker. The characteristic wavelength λ is 1.54 Å (Cu Kα radiation), and all samples were scanned with the 2θ range from 5° to 75°.

2.5. Gas permeation tests

Mixed gas permeation experiments were conducted by an in-house permeation setup reported elsewhere. [22, 23] The CO_2/N_2 (10/90 v/v%) gas mixture was employed as the feed gas, whereas the sweep gas was pure CH_4. The sweep pressure was kept around 1 bar, while the feed pressure was adjusted based on the required test conditions. The operating temperatures were controlled by a ventilated oven, inside which a larger part of the gas permeation setup was mounted. The compositions of both permeate and retentate streams were real-time monitored by a gas chromatograph (490 Micro GC, Agilent). The gas permeability (P_i) of the *i*th penetrant species is calculated using equation (1):

$$P_i = \frac{N_{perm} y_i L}{A\left(p_{i,ret} - p_{i,perm}\right)} \quad (1)$$

where N_{perm} is the permeate flow measured by a bubble flow meter (mL/min), y_i is the molar fraction of the gas *i* in the permeate flow (%), *L* represents the membrane thickness (μm), $p_{i,ret}$ and $p_{i,perm}$ stand for the partial pressures of the gas *i* in retentate and permeate streams (bar), respectively, and *A* is the effective membrane area (cm^2). In the present work, the unit of gas permeability is Barrer (1 Barrer = 10^{-10} cm^3(STP)*cm*cm^{-2}*s^{-1}*$cmHg^{-1}$). The separation factor was determined from equation (2):

$$\alpha_{ij} = \frac{y_i/y_j}{x_i/x_j} \quad (2)$$

where y_i and y_j are the mole ratio of gas *i* and *j* in permeate stream, respectively, while x_i and x_j present the mole ratio of gas *i* and *j* in the retentate side, respectively.

All permeation test data were the average values obtained by testing at least two membrane samples with the difference within 10% between the test values. The membrane thickness for each membrane sample was averaged from more than 10 measurements to ensure the accuracy.

3. Results and discussion

3.1.Properties and morphology studies of ZIFs

Three ZIFs with different shapes were fabricated with the same Hmim/Zn^{2+} ratio in aqueous solution at room temperatures. It is well known that additives play an important role in crystal formation and the growth of the inorganic crystals, and then tune the ZIFs' morphologies, like shapes and sizes.[21, 24] The crystals of the ZIFs generated in PEG solution have a rhombic dodecahedron appearance with a size of around 2 μm, as shown in **Figure 1 (A)**. While the ones generated from PVA 89-98 solution are sharp needles with a length of 6 μm and a width of 0.6 μm (as shown in **Figure 1(B)**). On the other hand, the 2D ZIF has a leaf-like shape (1.3 × 5.4 μm, shown in **Figure 1(C)**), in agreement with a previous report. [25] In addition to the differences in the shapes of the fillers, the XRD characterization results suggests that the crystal structure of these three ZIFs are not the same. The XRD pattern of 1D ZIF matches that of leaf ZIF-L, which is the 2D ZIF in this work. This suggests that the existence of PVA during ZIF synthesis seems to have a negligible effect on the crystal structure.[21] Unexpectedly, the 0D ZIF has similar XRD pattern with ZIF-8, [26] despite having the same Him/Zn^{2+} ratio (8:1) as ZIF-L [25], which is much lower than the typical ratio for synthesizing ZIF-8 particles (70:1). [27] It is well-known that the Him/Zn^{2+} ratio has great impact on the crystal structure of the resultant particles, especially in aqueous solutions. [28] While the presence of PEG seems to stabilize the Him-Zn coordination structure and allows for the formation of ZIF-8 at low Him/Zn^{2+} ratio.[29]

TGA was employed to investigate the thermal stabilities of the ZIF. As shown in **Figure 1 (E)**, all the samples lost a small amount of H_2O when the temperature reaches around 100 ^oC. With increasing temperature, the 0D and 1D ZIF starts decomposing, followed by the 2D ZIF. The relatively lower thermal stability of the ZIFs synthesized in polymeric solution is probably due to the polymeric chains entangling with the crystal cells. The ZIF formed in additive-free condition has relatively higher decomposition temperature. During this stage, the loss in weight mainly comes from the losing the structural water molecules and unreacted compounds. [27] All the samples presented a significant weight loss within the temperature range of 200 -300 ^oC. The 0D ZIF has relatively smaller slop, which is mainly due to the decomposition of the ligand. Afterwards, the residual masses of these three ZIFs remain almost unchanged with increasing temperature, indicating that the crystal structure of the ZIFs have been destroyed and changed to the ZnO form. [30, 31] FTIR spectroscopy was also used to analyze the chemical composition of the as-synthesized ZIFs and the results are presented in **Figure 1 (F)**. Since the ionic bonds cannot be detected by FTIR, the only bonding observed are those in Hmim molecules, like C-N and C=N bonds, which has characteristic peaks around 1310 and 1130 cm^{-1}, and 1568 cm^{-1}, [32, 33] respectively. These peaks are clearly noticed in the spectra of the three ZIFs, suggesting the presence of organic linkers. Combined with other characterization results, these as-synthesized ZIFs' crystal cells are composed of the Hmim and Zn^{2+}, but in different construction ways.

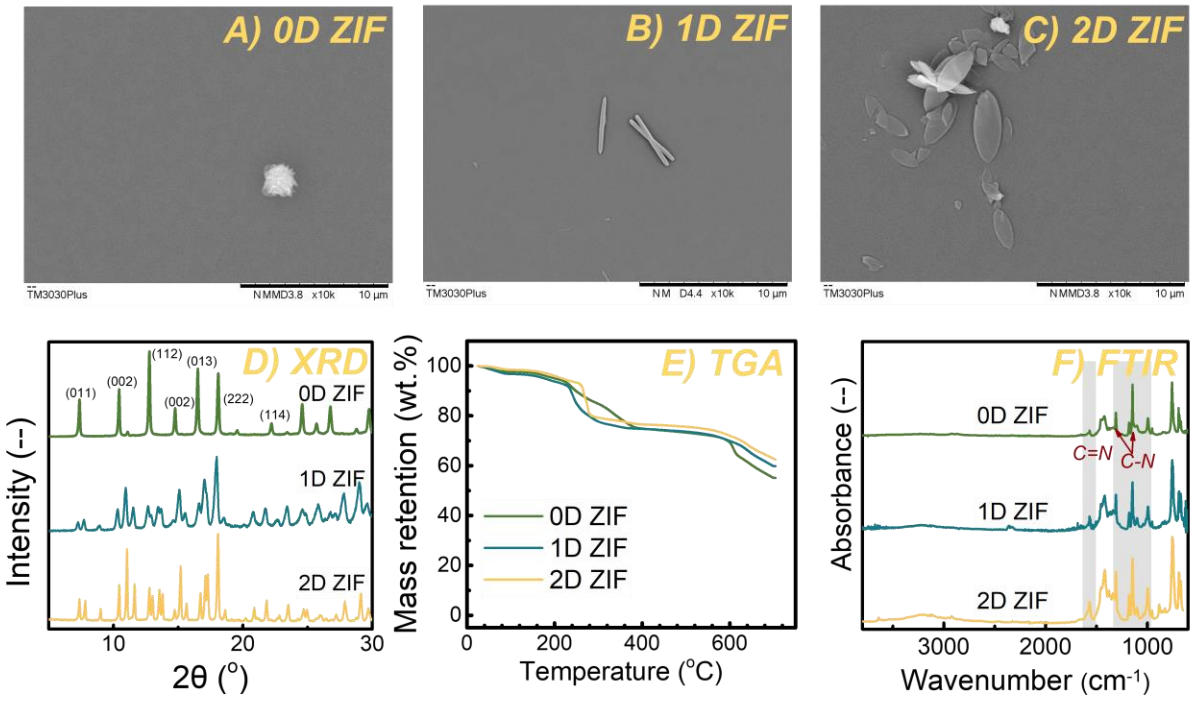

Figure 1 The SEM images of A) 0D ZIF, B) 1D ZIF and C) 2D ZIF, and D) XRD curves, E) TGA results and F) the FTIR spectra of these ZIFs.

3.2.Properties and morphology studies of MMMs

3.2.1. Chemical property

The FTIR spectroscopy was employed to analyze the chemical properties of the Pebax 2533 + 1D ZIFs MMM and the results are presented in **Figure 2** and **Figure S1**. The peaks located around 3300 cm^{-1}, 1640 cm^{-1} and 1100 cm^{-1} are associated with the amine (N-H) in polyamide segments, carbonyl (C=O) and ether (C-O) groups in polyether chains, respectively. This matches with the chemical structure of the neat Pebax 2533 and peak information in the previous literature. [34, 35] For the MMMs containing ZIFs, these aforementioned peaks become weaker with increasing ZIF loadings, as shown in **Figure 2 (A)**, due mainly to the decreasing Pebax content inside the membranes. On the other hand, the intensity of the peak corresponding to ZIFs (1310 cm^{-1}) increases with the addition of the ZIF, as shown in **Figure 2 (B)**. It is worth noting that no new

peaks or peak shifting has been observed. These results suggest that the ZIFs indeed were physically blended into the Pebax matrix as expected.

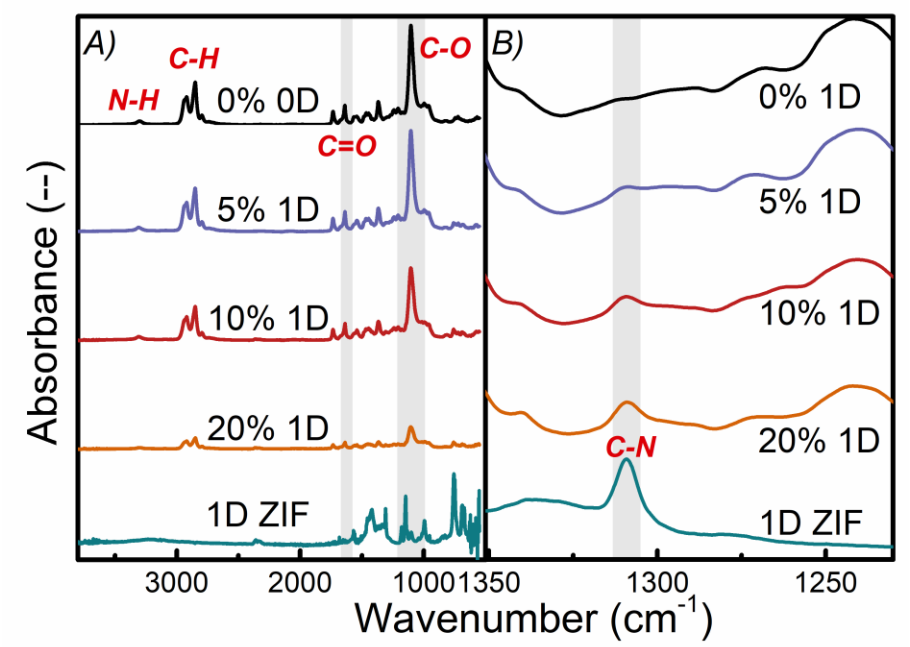

Figure 2 The FTIR spectra of the MMMs containing 1D ZIFs with a range of A) 4000 – 500 cm^{-1} and B) 1350 – 1230 cm^{-1}

3.2.2. Thermal properties

The thermal characterizations are very important and useful in understanding the hybrid materials and thus their properties. The thermal stability of MMMs were investigated by TGA, and the results are shown in **Figure 3** and **S3**. The neat Pebax 2533 has single-stage decomposition behavior with a T_{onset} of ~ 370 ^{o}C, which is much higher than those of the three ZIFs used in the current study. Naturally, adding ZIFs results in left-shifted decomposition temperature of the MMMs, despite the ZIFs' morphologies. With increasing ZIF loading in MMMs, the T_{onset} of the hybrid materials decreases and the residual mass increases, as shown in **Figure 4**, indicating that the actual amount of ZIFs in MMMs is increasing as expected. In addition to the changes in T_{onset}, the decomposition behavior of the MMMs is also affected by the ZIFs: the one-step decomposition

curve turns to multi-stage curves. The low filler loading leads to at least three stages: 300 ~ 330 °C, 330 ~ 360 °C and 360 ~ 470 °C, which corresponds to the ZIFs and Pebax 2533 chains, respectively. The higher loading causes less clear boundaries between stages.

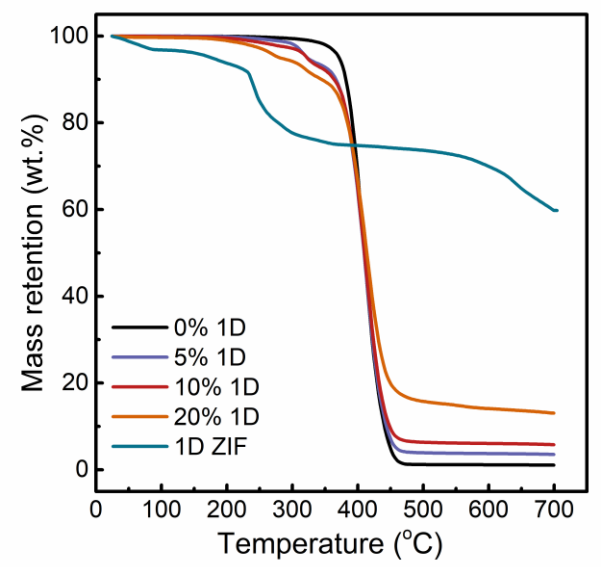

Figure 3 The TGA results of the MMMs with various loading of 1D ZIFs.

In addition, DSC was also employed to characterize the MMMs, and the second heating curve of the different membranes are displayed in **Figure 4** and **S4**. Two distinct peaks are observed in all curves: one located around 15 °C and the other near 138 °C. Considering the chemical structure of the Pebax 2533, the peak around 15 °C is believed to be the melting peak of the soft PEO chains, while the second one belongs to the hard PA segment, which are in good agreement with the results previously reported. [35-37] In addition to the melting temperatures, the peak area is theoretically related to the amount of required heat during melting process, which is proportional to content of the corresponding compound. Firstly, for neat Pebax 2533, the melting peak of PEO segment is much bigger than the one of PA blocks, which agrees with the composition of Pebax 2533 (86 mol% PE and 14 mol% PA). [34] Secondly, with incorporating ZIFs, both melting peaks become increasingly smaller, and the T_m of the PA blocks shifts to lower values, which indicate the

decreasing amount of the polymeric chains in the MMMs. In addition to the influences of the fillers' content, the morphology of the fillers also has influences on the final thermal properties. The MMMs containing 20 wt.% 0D and 1D ZIF have T_ms of PA segment around 132 °C, while the T_m of the one with 2D decreases to 126 °C. The lower melting temperature may be because the leaf 2D ZIF could break the PA zones and thus interrupt the formation of crystalline zones, [38] leading to less required energy for melting the crystalline and the amorphous chains.

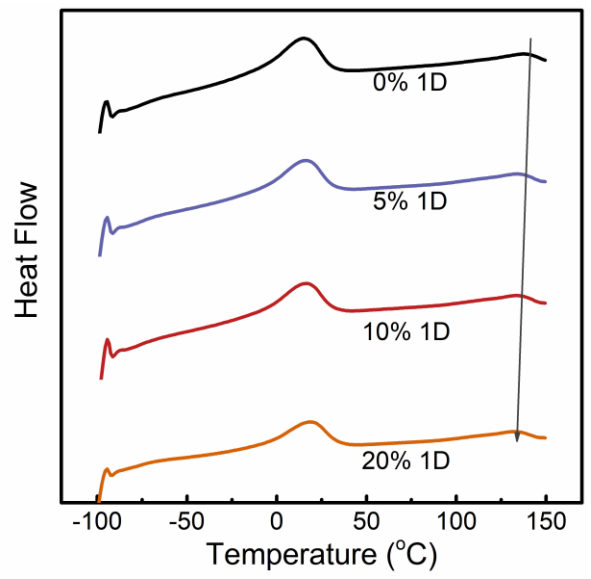

Figure 4 The DSC results of the MMMs with various loading of 1D ZIFs.

3.2.3. Crystallinity

Crystallization has great influence on the various properties of the polymers, such as mechanical properties and gas separation performance. XRD tests were performed for all MMMs and the neat Pebax 2533 membranes as shown in **Figure 5** and **S5**. The neat polymer membrane has two broad peaks locating at 11.7° and 19.8°, respectively, corresponding to the semi-crystalline nature of the Pebax 2533. [39-41] On the other hand, incorporating the highly crystalline materials introduces the sharp and narrow peaks originating from the ZIFs and shrinks the broad peaks of the Pebax 2533.

Meanwhile, with the increasing ZIF loading, the sharp peaks become more obvious while these amorphous peaks diminish significantly. This presents the increasing content of ZIF and the decreasing amount of Pebax in these MMMs, greatly agreeing with previous FTIR characterization results. It is worth noting that the peaks at ~ 29° present in all membrane samples but not in the ZIF powder, which are most likely from the vacuum grease used to mounter membrane sample.

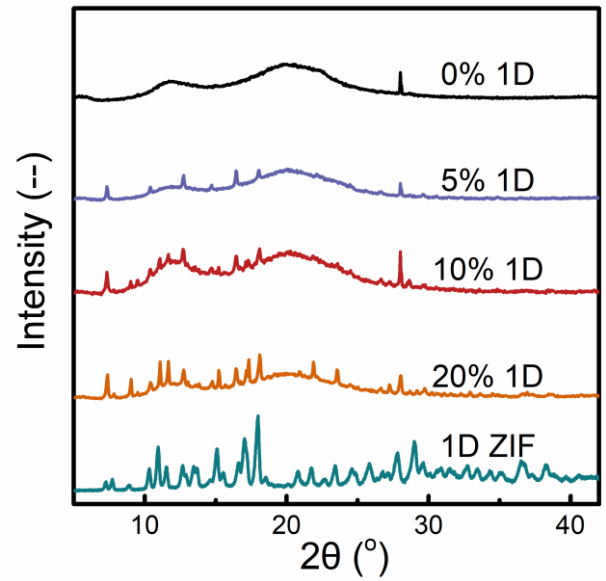

Figure 5 The XRD results of the MMMs with various loading of 1D ZIFs.

3.2.4. Morphology study

As discussed previously, the incorporation of inorganic fillers into the polymeric matrix may cause unideal dispersion in the resultant MMMs, which may be observed by a SEM. The surface and cross-section images of all Pebax + ZIF MMMs are presented in **Figure 6** and **S6.** The neat polymeric membranes have smooth surfaces and void-free cross-sections (**Figure 6 (A)**). While the surfaces and cross-sections of all MMMs become rougher with increasing filler contents, despite the morphology of the ZIFs. Moreover, based on these SEM images, all the three ZIFs seems to be dispersed well in the resultant MMMs and no obvious aggregation of ZIFs has been

seen, except for the one containing 20 wt.% 2D ZIF. The membranes with 20 wt.% 2D ZIF clearly have phase-separation from both surface and cross-section images, due probably to the 2D ZIF aggregation during membrane fabrication. The reason for this much higher agglomeration trend of 2D ZIF is probably its leaf-like shape, compared to the other ZIFs studied in the current work. It is well-known that inorganic fillers tend to aggregate at high filler loadings, and many factors could lead to this unpleasant result, such as particle size, bad compatibility with the polymeric matrix and the shape of the fillers. Several research works have reported that for inorganic fillers with high aspect ratio (> 10), a low loading may be more attractive [42] because of the greater possibility of stack and aggregation. Moreover, they could offer the same or even better performances at lower loadings compared to the typical spheres.

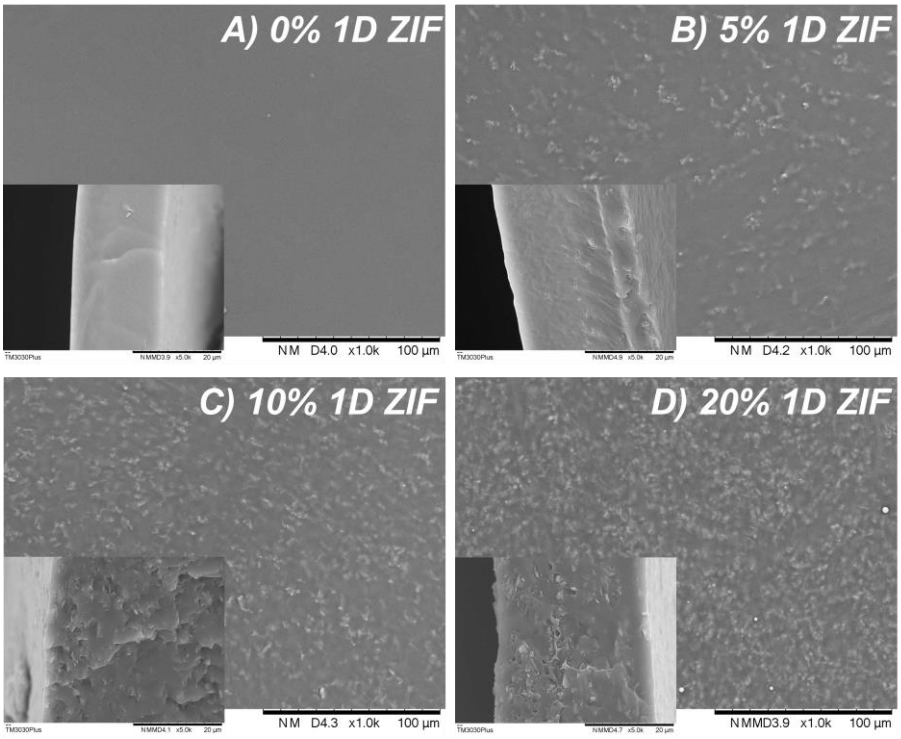

Figure 6 The SEM images of the MMMs containing 1D ZIFs with various loading.

3.2.5. Permeation study

Effect of filler

The CO_2/N_2 separation performance of the resultant MMMs with three ZIFs fillers was evaluated by the mixed gas permeation tests at room temperature with a feed pressure of 2 bar. The CO_2 permeability and CO_2/N_2 separation factor of the resultant MMMs as a function of filler content are presented in **Figure 7**.

The neat Pebax 2533 have a CO_2 permeability of ~ 220 Barrer with a CO_2/N_2 separation factor of 26, in good agreement with previously reported values.[43-47] A clear increment in CO_2 permeability was observed with the addition of all ZIF fillers, despite the difference in particle shapes. This enhancement may be explained by several factors. First, the addition of ZIFs disrupts the packing way of polymeric chains and then rises the free volume of the resultant membranes. Meanwhile, the pores of these ZIFs act as molecular sieves, allowing the small specimens, like CO_2 in the current work, pass through but not the big ones, which offers the extra transport paths for CO_2 and hence benefiting their permeabilities. However, further increasing the ZIF loading has negative effects on the CO_2 permeability, probably due to the increasing degree of filler aggregation in the nano-scale, [48, 49] although this level of aggregation was not observed by microscopy. Despite this similar trend, there exists some difference between the influences of adding each ZIF. The optimal ZIF loadings are related to the morphologies of the employed ZIF: the peaks are located at 10 wt.% for 0D and 1D, while 5 wt.% for 2D. Several researches have inferred that the high aspect ratio of 2D nanomaterials endows similar or better performance at lower loading compared to the spherical ones, the most common filler shape, [20, 50, 51] in accordance with the results of the current work. It is worth mentioning that the membrane with 5 wt.% 2D ZIF has the highest CO_2 permeability

(425.0 Barrer), followed by the one with 10 wt.% 1D ZIF (411.4 Barrer) and 0D ZIF (376.7 Barrer). Moreover, the reason of that the membranes containing 1D ZIFs is more permeable than that with 0D ZIF at same loading is probably because that the interface between the polymeric matrix and microneedles is slightly better than that between the polymeric materials with the micro-particles. One of our previous studies found that the ZIFs synthesized in PVA solutions may entangle with PVA chains during the formation of crystal cells, and as a result, achieve good compatibility with Pebax. [21] This may be one of the reasons the microneedle-shaped ZIFs, prepared in PVA solution, have better interfaces with Pebax phase.

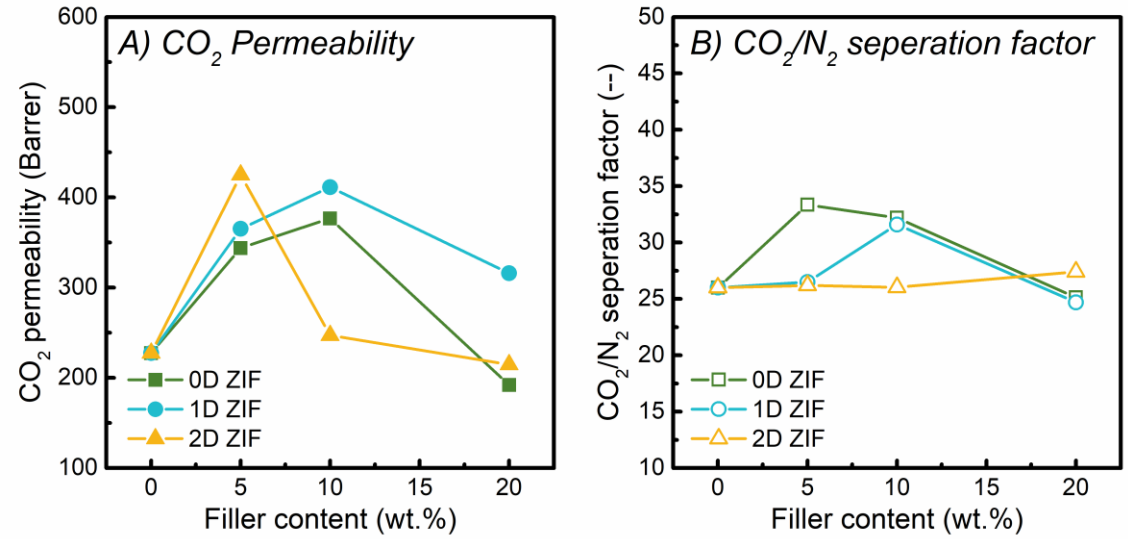

Figure 7 The A) CO_2 permeability and B) CO_2/N_2 separation factor of the MMMs with different filler loading (tested at dry condition and room temperature with a feed pressure of 2 bar).

In addition to the gas permeability, the ZIFs' morphologies also play a role in the CO_2/N_2 separation factor (as shown in **Figure 7 (B)**). The incorporation of 0D or 1D into Pebax lifts the CO_2/N_2 selectivity from 26 to above 30. The presence of ZIFs leads to more tortuous transport paths for larger gases, while in the meantime, the pores inside these ZIFs may work as molecular sieves, allowing the small CO_2 to pass through. Therefore, the selectivity is reinforced by adding ZIFs. However, further addition provokes deterioration, as a result of filler aggregation. On the

other hand, the CO_2/N_2 separation factor of membranes with 2D ZIFs stay almost unchanged. This probably is because the interfaces between Pebax and 2D ZIF is not ideal, which generates the non-selective gaps (sieve-in-a-cage) and then fails to improve the selectivity at low loading. At high loading, the ZIFs agglomerate, as shown in SEM image (**Figure S6 (H)**) and thus fail separating gas mixtures. It is worth mentioning that despite the different crystal structure of 0D ZIF with 1D or 2D ZIFs as indicated by the XRD results, the differences in gas separation performances of the resulting MMMs may be insignificant considering the same chemical properties of all ZIFs and the similar gas absorption results of the pure ZIF-8 and ZIF-L, as reported by Wang et. al..[25]

These aforementioned performances were compared with the 2008 upper bound, as shown in **Figure 8.** The MMMs with 0D and 1D ZIF move towards the upper right corner, while the membrane with 5 wt.% 2D ZIF only shifts towards the right side. For the Pebax 2533 + 0D ZIF membrane, although increasing filler content decreases the selectivity, the membrane with 10% 0D filler are equally close to the Upper Bound with the one containing 5% filler due to the higher gas permeability. In general, the incorporation of these ZIFs does push the separation performance closer to the upper bound, but still cannot surpass it. Considering the improved performances, three membranes (10% 0D, 10% 1D and 5% 2D ZIF) with performances close to the upper bound were chosen for further study.

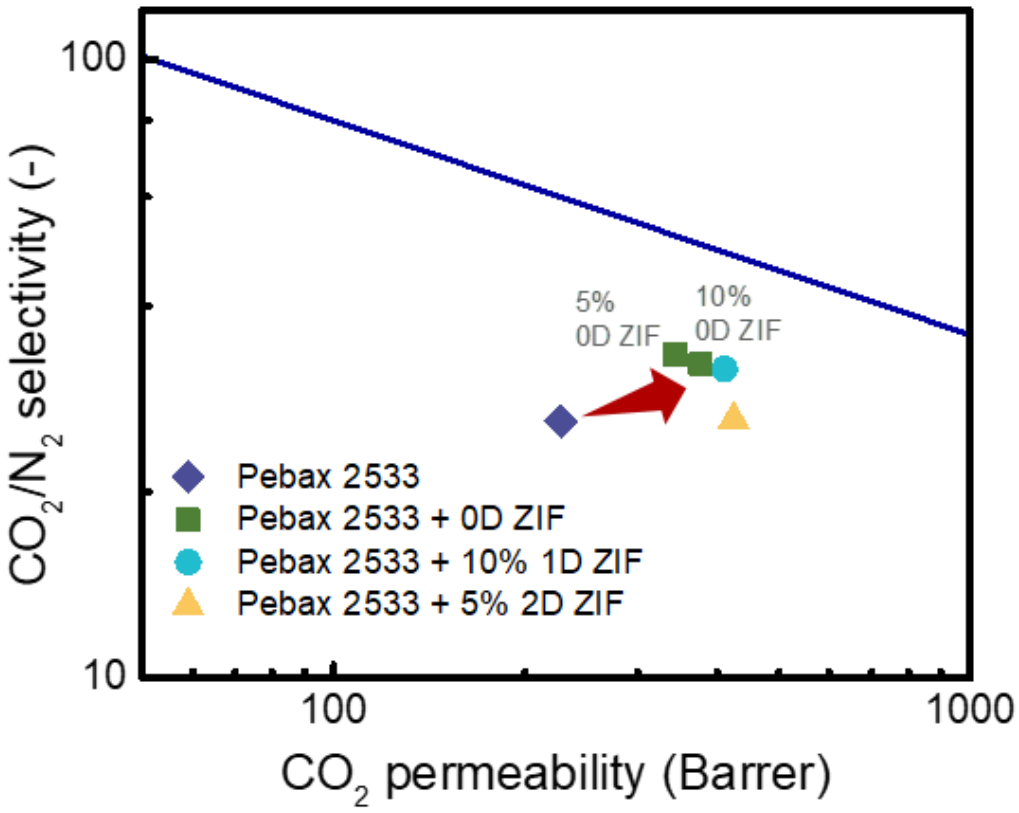

Figure 8 Comparison of the CO_2/N_2 separation performance of Pebax + ZIFs membranes with the 2008 Upper bound.

Effect of operating temperature

The effects of the operating temperature have been investigated by conducting mixed gas permeation experiments at different temperatures: 24, 40 and 60 ^oC (**Figure 9**). The CO_2 permeabilities of all membranes increase significantly, while the CO_2/N_2 separation factors decrease with increasing operating temperature. The higher operating temperature facilitates the diffusion of gas molecules, which benefits the enhancement in gas permeability. Moreover, the polymeric chains become more flexible at higher temperatures, and then form more free volume for gas transporting through membranes, consequently leading to higher gas permeability. While the increment in CO_2 permeability with the increasing temperature seems to be negatively affected by the added ZIFs, indicating by the less slope of the membranes containing ZIFs compared to the

neat Pebax. The presence of ZIFs inside membranes may hinder the chain mobility at higher temperature, and hence results in less increments in gas permeability. Among them, the 2D ZIF seems to have more influence on the polymeric chain packing because of its greater decrease in CO_2 permeability.

On the other hand, for most of polymeric membranes, increasing operating temperatures usually leads to decreasing CO_2/light gas selectivity, as a result of the wider pore element distribution at higher temperature. This agrees with the results of neat Pebax, as illustrated in **Figure 9 (B)**. For the membranes containing ZIFs, the separation factors also decrease, as expected, since the Pebax still is the main ingredient (90 or 95 %) of these MMMs. In addition, the loss in the CO_2/N_2 separation factor of these four membranes are similar, which at 60 ^oC, only have remained 50% of the values at R.T.. Therefore, it could be concluded that these decreases are mainly caused by the behavior of the neat Pebax.

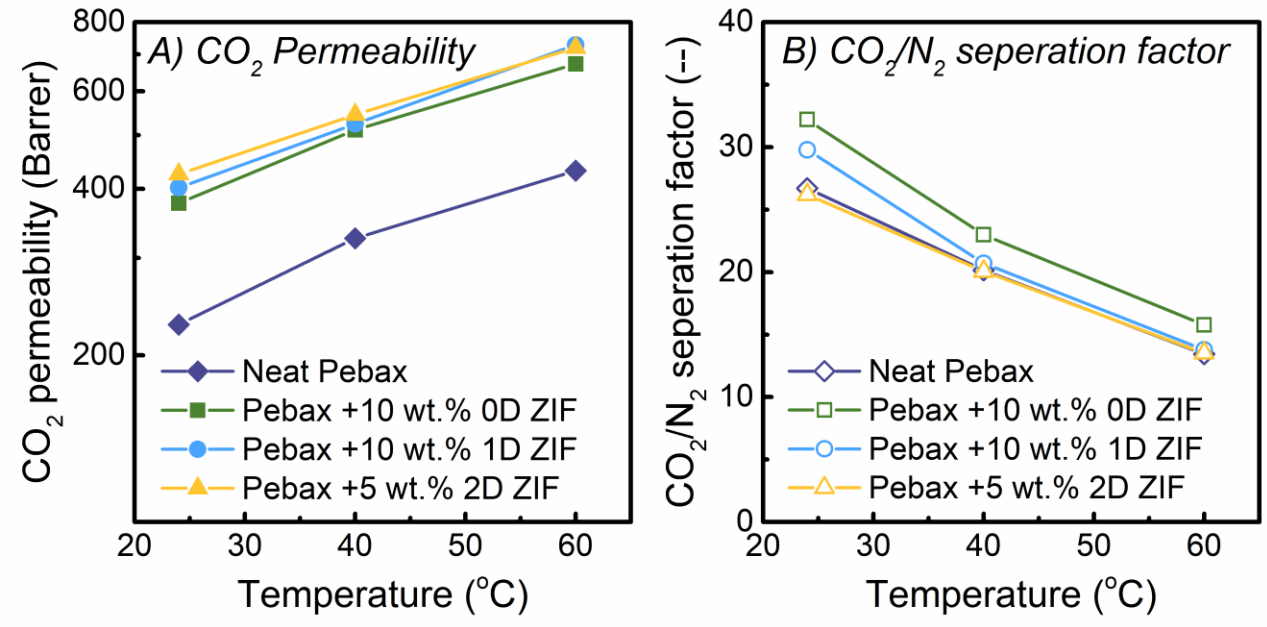

Figure 9 The A) CO_2 permeability and B) CO_2/N_2 separation factor of the MMMs as a function of operation temperature. (Tested at dry condition with a feed pressure of 2 bar.)

Effect of feed pressure

The influences of the feed pressure were also studied, and the results are presented in **Figure 10**. The CO_2 permeability and the CO_2/N_2 separation factor of the neat Pebax membrane decrease slightly (~ 5%) with the increasing feed pressure, in consistence with the previous studies. [52, 53] One possible reason is that the feed pressure compresses the polymeric chains and then reduces the free volume, and consequently the CO_2 permeability. [42] For the MMMs, the decrease rate of CO_2 permeability is close to that of the neat Pebax, while the changes in CO_2/N_2 separation factor seem largely dependent on the types of fillers. The membrane with 0D ZIF has almost unchanged selectivity with increasing feed pressure. However, the CO_2/N_2 selectivity of the membrane containing 10% 1D ZIF reduces from 28 to 14 when feed pressure increases from 2 bar to 6 bar. Membranes containing 1D ZIFs are much less robust compared to the neat Pebax membrane: the pore elements generated by adding ZIFs may merge together thus reduce the molecular-sieving effect at higher operation pressures. This result indicates that the Pebax + 1D ZIF membranes may not be a good candidate for high pressure application. Unexpectedly, the Pebax + 10% 0D ZIF membranes have better resistance to the feed pressure compared to the other two MMMs in terms of CO_2/N_2 selectivity.

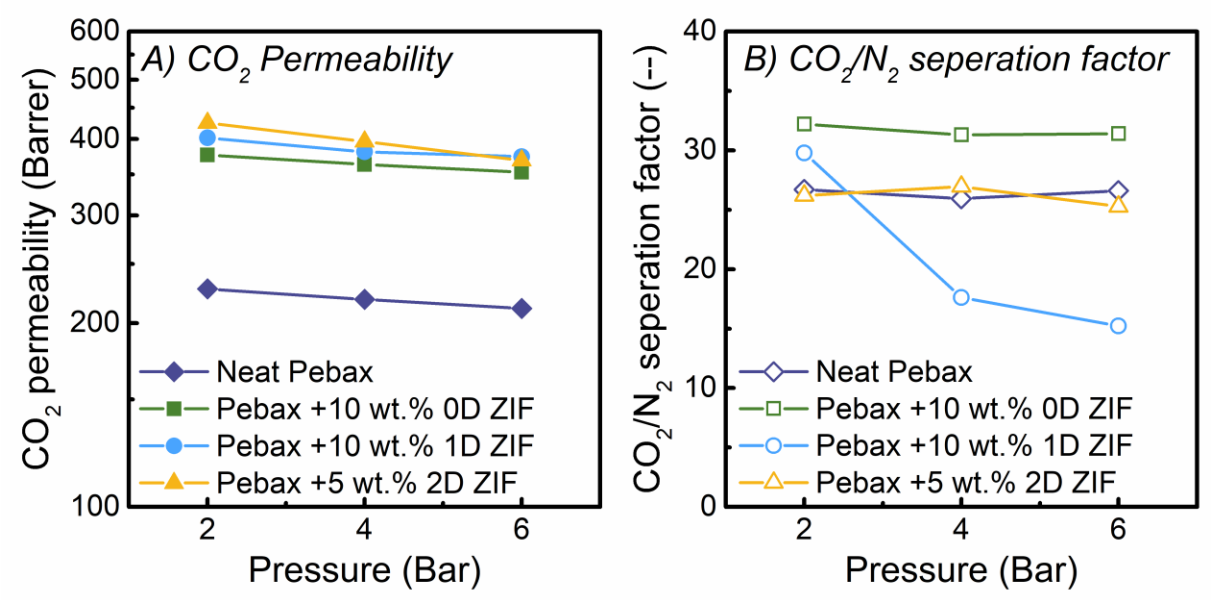

Figure 10 The A) CO_2 permeability and B) CO_2/N_2 separation factor of the MMMs with a function of feed pressure. (Tested at dry condition and room temperature)

4. Conclusions

In present work, three ZIFs with three different morphologies (particles, microneedles and leaves) were prepared. The presence of polymeric additives (PEG 400 and PVA) play an important role on the construction and the structures of the ZIF crystals. The characterization results indicate that the ZIF particles synthesized in PEG 400 solution have the same crystal structure with ZIF-8, while the microneedle-shaped ZIF from PVA solution is closer to that of the 2D ZIF, although the shapes of the fillers are quite different.

The influence of the ZIFs with different morphology on the Pebax 2533 + ZIF MMMs were systemically evaluated by several characterization approaches. The chemical, thermal and the crystalline properties of the resultant MMMs have proved the presence of the aforementioned ZIFs, indicating the successful incorporation of ZIFs into Pebax matrix. Further morphology analysis also confirms the well-dispersion of these fillers inside the MMMs at low ZIF loading, based on

both surface and cross-section images. However, the addition of 20 wt.% 2D ZIF leads to clear agglomeration, while the aggregation in the samples of 0D or 1D fillers is not observed from their SEM images.

The mixed gas permeation results show that the incorporation of these ZIFs firstly increases and then decreases the CO_2 permeability, regardless of the morphology of the filler. But the optimal ZIF contents are dependent on the filler morphology: 10 wt.% for 0D and 1D ZIF, while 5 wt.% for 2D. Similar influences of the filler loading were found for the CO_2/N_2 selectivity of the membranes with 0D or 1D ZIFs, and the optimal ZIF loadings for selectivity are the same as those for CO_2 permeability. Moreover, the comparison of the best CO_2 separation performance among the three MMMs shows that the increment in CO_2 permeability is associated with the ZIFs' morphologies in the order: 0D < 1D < 2D, despite the lower loading of 2D ZIFs. An opposite trend was observed for CO_2/N_2 selectivity. Therefore, three optimized MMMs were chosen to study the effects of the operating temperature and the feed pressure. The increasing operating temperature results in greatly enhanced CO_2 permeability and reduced CO_2/N_2 selectivity for all membranes, while this difference in the impact on the operating temperature for the investigated MMMs are similar to that of neat Pebax membrane. The highest CO_2 permeability is endowed by the Pebax 2533 + 10% 1D ZIF membrane at 60 ^{o}C with a decreased CO_2/N_2 selectivity. The change in feed pressure results in a different behavior: the membranes containing 0D or 2D ZIF display a decreased gas permeability and almost unchanged gas selectivity with increasing feed pressure, a classical behavior of polymeric membrane. While in terms of the one with 1D ZIF, the CO_2/N_2 selectivity deteriorates largely (reduced almost by 50 %). Hence, in this work, the 0D ZIF may be the most promising fillers in Pebax 2533 matrix, especially for high pressure CO_2/N_2 separation.

ASSOCIATED CONTENTS

SUPPORTING INFORMATION

The results of FTIR, TGA, DSC, XRD and SEM images of membranes containing 0D and 2D ZIF were presented in Supporting Information.

AUTHOR INFORMATION

Corresponding Author

* Liyuan Deng.

E-mail: deng@nt.ntnu.no, Tel.: +47 73594112,

ORCID:

Zhongde Dai: 0000-0002-3558-5403

Jing Deng: 0000-0003-3680-3799

Liyuan Deng: 0000-0003-4785-4620

Author Contributions

ZD developed and characterized the nanofiller, and JD fabricated, tested and characterized the MMMs. The manuscript was written through contributions of all authors. All authors have given approval to the final version of the manuscript.

Notes

The authors declare no competing financial interest.

ACKNOWLEDGEMENTS

This work is supported by the Research Council of Norway through CLIMIT program ("POLYMEM" project, No. 254791).

REREFENCES

1. Wu, Z., Inorganic Membranes for Gas Separations. In *Membrane Separation Principles and Applications*, Ismail, A. F.; Rahman, M. A.; Othman, M. H. D.; Matsuura, T., Eds. Elsevier: 2019; pp 147-179.
2. Kim, J. F.; Jung, J. T.; Wang, H. H.; Lee, S. Y.; Moore, T.; Sanguineti, A.; Drioli, E.; Lee, Y. M., Microporous PVDF membranes via thermally induced phase separation (TIPS) and stretching methods. *Journal of Membrane Science* **2016,** 509, 94-104.
3. Zhu, L.; Yin, D.; Qin, Y.; Konda, S.; Zhang, S.; Zhu, A.; Liu, S.; Xu, T.; Swihart, M. T.; Lin, H., Sorption-Enhanced Mixed Matrix Membranes with Facilitated Hydrogen Transport for Hydrogen Purification and CO_2 Capture. *Advanced Functional Materials* **2019,** 29, (36), 1904357.
4. Cheng, Y.; Wang, Z.; Zhao, D., Mixed Matrix Membranes for Natural Gas Upgrading: Current Status and Opportunities. *Industrial & Engineering Chemistry Research* **2018,** 57, (12), 4139-4169.
5. Ding, Y., Perspective on Gas Separation Membrane Materials from Process Economics Point of View. *Industrial & Engineering Chemistry Research* **2020,** 59, (2), 556-568.
6. *Gas Separation Membranes Market by Material type (Polyimide & Polyaramide, Polysulfone, and Cellulose Acetate), Application (Nitrogen Generation & Oxygen Enrichment, Carbon Dioxide Removal, and Hydrogen Recovery), and Region - Global Forecast to 2024*; MarketsandMarkets™: 2019.
7. Robeson, L. M., The upper bound revisited. *Journal of membrane science* **2008,** 320, (1-2), 390-400.
8. Seoane, B.; Coronas, J.; Gascon, I.; Etxeberria Benavides, M.; Karvan, O.; Caro, J.; Kapteijn, F.; Gascon, J., Metal-organic framework based mixed matrix membranes: a solution for highly efficient CO_2 capture? *Chem Soc Rev* **2015,** 44, (8), 2421-54.
9. Galizia, M.; Chi, W. S.; Smith, Z. P.; Merkel, T. C.; Baker, R. W.; Freeman, B. D., 50th Anniversary Perspective: Polymers and Mixed Matrix Membranes for Gas and Vapor Separation: A Review and Prospective Opportunities. *Macromolecules* **2017,** 50, (20), 7809-7843.
10. Wang, Y.; Wang, X.; Guan, J.; Yang, L.; Ren, Y.; Nasir, N.; Wu, H.; Chen, Z.; Jiang, Z., 110th Anniversary: Mixed Matrix Membranes with Fillers of Intrinsic Nanopores for Gas Separation. *Industrial & Engineering Chemistry Research* **2019,** 58, (19), 7706-7724.
11. Song, Q.; Nataraj, S.; Roussenova, M. V.; Tan, J. C.; Hughes, D. J.; Li, W.; Bourgoin, P.; Alam, M. A.; Cheetham, A. K.; Al-Muhtaseb, S. A., Zeolitic imidazolate framework (ZIF-8) based polymer nanocomposite membranes for gas separation. *Energy & Environmental Science* **2012,** 5, (8), 8359-8369.
12. Shen, J.; Liu, G.; Huang, K.; Jin, W.; Lee, K.-R.; Xu, N., Membranes with Fast and Selective Gas-Transport Channels of Laminar Graphene Oxide for Efficient CO_2 Capture. *Angewandte Chemie* **2015,** 127, (2), 588-592.

13. Lin, R.; Villacorta Hernandez, B.; Ge, L.; Zhu, Z., Metal organic framework based mixed matrix membranes: an overview on filler/polymer interfaces. *Journal of Materials Chemistry A* **2018,** 6, (2), 293-312.
14. Ayas, İ.; Yilmaz, L.; Kalipcilar, H., The Gas Permeation Characteristics of Ternary Component Mixed Matrix Membranes Prepared Using ZIF-8 with a Large Range of Average Particle Size. *Industrial & Engineering Chemistry Research* **2018,** 57, (47), 16041-16050.
15. Sánchez-Laínez, J.; Zornoza, B.; Friebe, S.; Caro, J.; Cao, S.; Sabetghadam, A.; Seoane, B.; Gascon, J.; Kapteijn, F.; Le Guillouzer, C.; Clet, G.; Daturi, M.; Téllez, C.; Coronas, J., Influence of ZIF-8 particle size in the performance of polybenzimidazole mixed matrix membranes for pre-combustion CO_2 capture and its validation through interlaboratory test. *Journal of Membrane Science* **2016,** 515, 45-53.
16. Bae, T.-H.; Lee, J. S.; Qiu, W.; Koros, W. J.; Jones, C. W.; Nair, S., A High-Performance Gas-Separation Membrane Containing Submicrometer-Sized Metal–Organic Framework Crystals. *Angewandte Chemie International Edition* **2010,** 49, (51), 9863-9866.
17. Japip, S.; Xiao, Y.; Chung, T.-S., Particle-Size Effects on Gas Transport Properties of 6FDA-Durene/ZIF-71 Mixed Matrix Membranes. *Industrial & Engineering Chemistry Research* **2016,** 55, (35), 9507-9517.
18. Zheng, W.; Ding, R.; Yang, K.; Dai, Y.; Yan, X.; He, G., ZIF-8 nanoparticles with tunable size for enhanced CO_2 capture of Pebax based MMMs. *Separation and Purification Technology* **2019,** 214, 111-119.
19. Sabetghadam, A.; Seoane, B.; Keskin, D.; Duim, N.; Rodenas, T.; Shahid, S.; Sorribas, S.; Le Guillouzer, C.; Clet, G.; Tellez, C.; Daturi, M.; Coronas, J.; Kapteijn, F.; Gascon, J., Metal Organic Framework Crystals in Mixed-Matrix Membranes: Impact of the Filler Morphology on the Gas Separation Performance. *Adv Funct Mater* **2016,** 26, (18), 3154-3163.
20. Rodenas, T.; Luz, I.; Prieto, G.; Seoane, B.; Miro, H.; Corma, A.; Kapteijn, F.; Llabrés i Xamena, F. X.; Gascon, J., Metal–organic framework nanosheets in polymer composite materials for gas separation. *Nature Materials* **2014,** 14, 48.
21. Deng, J.; Dai, Z.; Hou, J.; Deng, L., Morphologically Tunable MOF Nanosheets in Mixed Matrix Membranes for CO2 Separation. *Chem. Mater.* **2020**, 32, 10, 4174–4184
22. Dai, Z.; Aboukeila, H.; Ansaloni, L.; Deng, J.; Giacinti Baschetti, M.; Deng, L., Nafion/PEG hybrid membrane for CO_2 separation: Effect of PEG on membrane micro-structure and performance. *Separation and Purification Technology* **2019,** 214, 67-77.
23. Dai, Z.; Deng, J.; Peng, K.-J.; Liu, Y.-L.; Deng, L., Pebax/PEG Grafted CNT Hybrid Membranes for Enhanced CO_2/N_2 Separation. *Industrial & Engineering Chemistry Research* **2019,** 58, (27), 12226-12234.
24. Yang, F.; Mu, H.; Wang, C.; Xiang, L.; Yao, K. X.; Liu, L.; Yang, Y.; Han, Y.; Li, Y.; Pan, Y., Morphological Map of ZIF-8 Crystals with Five Distinctive Shapes: Feature of Filler in Mixed-Matrix Membranes on C_3H_6/C_3H_8 Separation. *Chemistry of Materials* **2018,** 30, (10), 3467-3473.
25. Chen, R.; Yao, J.; Gu, Q.; Smeets, S.; Baerlocher, C.; Gu, H.; Zhu, D.; Morris, W.; Yaghi, O. M.; Wang, H., A two-dimensional zeolitic imidazolate framework with a cushion-shaped cavity for CO_2 adsorption. *Chemical Communications* **2013,** 49, (82), 9500-9502.
26. Zhou, K.; Mousavi, B.; Luo, Z.; Phatanasri, S.; Chaemchuen, S.; Verpoort, F., Characterization and properties of Zn/Co zeolitic imidazolate frameworks vs. ZIF-8 and ZIF-67. *Journal of Materials Chemistry A* **2017,** 5, (3), 952-957.

27. Pan, Y.; Liu, Y.; Zeng, G.; Zhao, L.; Lai, Z., Rapid synthesis of zeolitic imidazolate framework-8 (ZIF-8) nanocrystals in an aqueous system. *Chemical Communications* **2011,** 47, (7), 2071-2073.
28. Kida, K.; Okita, M.; Fujita, K.; Tanaka, S.; Miyake, Y., Formation of high crystalline ZIF-8 in an aqueous solution. *CrystEngComm* **2013,** 15, (9), 1794-1801.
29. Fan, X.; Wang, W.; Li, W.; Zhou, J.; Wang, B.; Zheng, J.; Li, X., Highly Porous ZIF-8 Nanocrystals Prepared by a Surfactant Mediated Method in Aqueous Solution with Enhanced Adsorption Kinetics. *ACS Applied Materials & Interfaces* **2014,** 6, (17), 14994-14999.
30. Li, W.; Wu, X.; Liu, H.; Chen, J.; Tang, W.; Chen, Y., Hierarchical hollow ZnO cubes constructed using self-sacrificial ZIF-8 frameworks and their enhanced benzene gas-sensing properties. *New Journal of Chemistry* **2015,** 39, (9), 7060-7065.
31. Hwang, S.; Chi, W. S.; Lee, S. J.; Im, S. H.; Kim, J. H.; Kim, J., Hollow ZIF-8 nanoparticles improve the permeability of mixed matrix membranes for CO2/CH4 gas separation. *Journal of Membrane Science* **2015,** 480, 11-19.
32. Tian, Z.; Yao, X.; Ma, K.; Niu, X.; Grothe, J.; Xu, Q.; Liu, L.; Kaskel, S.; Zhu, Y., Metal–Organic Framework/Graphene Quantum Dot Nanoparticles Used for Synergistic Chemo- and Photothermal Therapy. *ACS Omega* **2017,** 2, (3), 1249-1258.
33. Wu, C.; Liu, Q.; Chen, R.; Liu, J.; Zhang, H.; Li, R.; Takahashi, K.; Liu, P.; Wang, J., Fabrication of ZIF-8@ SiO_2 micro/nano hierarchical superhydrophobic surface on AZ31 magnesium alloy with impressive corrosion resistance and abrasion resistance. *ACS applied materials & interfaces* **2017,** 9, (12), 11106-11115.
34. Armstrong, S.; Freeman, B.; Hiltner, A.; Baer, E., Gas permeability of melt-processed poly(ether block amide) copolymers and the effects of orientation. *Polymer* **2012,** 53, (6), 1383-1392.
35. Dai, Z.; Bai, L.; Hval, K. N.; Zhang, X.; Zhang, S.; Deng, L., Pebax®/TSIL blend thin film composite membranes for CO_2 separation. *Science China Chemistry* **2016,** 59, (5), 538-546.
36. Estahbanati, E. G.; Omidkhah, M.; Amooghin, A. E., Preparation and characterization of novel Ionic liquid/Pebax membranes for efficient CO_2/light gases separation. *Journal of Industrial and Engineering Chemistry* **2017,** 51, 77-89.
37. Guan, P.; Luo, J.; Li, W.; Si, Z., Enhancement of gas permeability for CH_4/N_2 separation membranes by blending SBS to Pebax polymers. *Macromolecular Research* **2017,** 25, (10), 1007-1014.
38. Dong, L.; Chen, M.; Wu, X.; Shi, D.; Dong, W.; Zhang, H.; Zhang, C., Multi-functional polydopamine coating: simultaneous enhancement of interfacial adhesion and CO_2 separation performance of mixed matrix membranes. *New Journal of Chemistry* **2016,** 40, (11), 9148-9159.
39. Dong, L.; Zhang, C.; Bai, Y.; Shi, D.; Li, X.; Zhang, H.; Chen, M., High-Performance PEBA2533-Functional MMT Mixed Matrix Membrane Containing High-Speed Facilitated Transport Channels for CO_2/N_2 Separation. *ACS Sustainable Chemistry & Engineering* **2016,** 4, (6), 3486-3496.
40. Han, J.; Bai, L.; Yang, B.; Bai, Y.; Luo, S.; Zeng, S.; Gao, H.; Nie, Y.; Ji, X.; Zhang, S.; Zhang, X., Highly Selective Oxygen/Nitrogen Separation Membrane Engineered Using a Porphyrin-Based Oxygen Carrier. *Membranes* **2019,** 9, (9).
41. Yu, S.; Jiang, Z.; Yang, S.; Ding, H.; Zhou, B.; Gu, K.; Yang, D.; Pan, F.; Wang, B.; Wang, S.; Cao, X., Highly swelling resistant membranes for model gasoline desulfurization. *Journal of Membrane Science* **2016,** 514, 440-449.

42. Zhu, W.; Li, X.; Sun, Y.; Guo, R.; Ding, S., Introducing hydrophilic ultra-thin ZIF-L into mixed matrix membranes for CO_2/CH_4 separation. *RSC Advances* **2019,** 9, (40), 23390-23399.
43. Bondar, V. I.; Freeman, B. D.; Pinnau, I., Gas transport properties of poly(ether-b-amide) segmented block copolymers. *Journal of Polymer Science Part B: Polymer Physics* **2000,** 38, (15), 2051-2062.
44. Gugliuzza, A.; Drioli, E., Evaluation of CO_2 permeation through functional assembled mono-layers: Relationships between structure and transport. *Polymer* **2005,** 46, (23), 9994-10003.
45. Tocci, E.; Gugliuzza, A.; De Lorenzo, L.; Macchione, M.; De Luca, G.; Drioli, E., Transport properties of a co-poly(amide-12-b-ethylene oxide) membrane: A comparative study between experimental and molecular modelling results. *Journal of Membrane Science* **2008,** 323, (2), 316-327.
46. Bernardo, P.; Jansen, J. C.; Bazzarelli, F.; Tasselli, F.; Fuoco, A.; Friess, K.; Izák, P.; Jarmarová, V.; Kačírková, M.; Clarizia, G., Gas transport properties of Pebax®/room temperature ionic liquid gel membranes. *Separation and Purification Technology* **2012,** 97, 73-82.
47. Scholes, C. A.; Chen, G. Q.; Lu, H. T.; Kentish, S. E., Crosslinked PEG and PEBAX Membranes for Concurrent Permeation of Water and Carbon Dioxide. *Membranes* **2016,** 6, (1).
48. Bachman, J. E.; Smith, Z. P.; Li, T.; Xu, T.; Long, J. R., Enhanced ethylene separation and plasticization resistance in polymer membranes incorporating metal–organic framework nanocrystals. *Nature Materials* **2016,** 15, 845.
49. Md. Nordin, N. A. H.; Ismail, A. F.; Mustafa, A.; Murali, R. S.; Matsuura, T., Utilizing low ZIF-8 loading for an asymmetric PSf/ZIF-8 mixed matrix membrane for CO_2/CH_4 separation. *RSC Advances* **2015,** 5, (38), 30206-30215.
50. Johnson, J. R.; Koros, W. J., Utilization of nanoplatelets in organic–inorganic hybrid separation materials: Separation advantages and formation challenges. *Journal of the Taiwan Institute of Chemical Engineers* **2009,** 40, (3), 268-275.
51. Karunakaran, M.; Shevate, R.; Kumar, M.; Peinemann, K. V., CO_2-selective PEO–PBT (PolyActive™)/graphene oxide composite membranes. *Chemical Communications* **2015,** 51, (75), 14187-14190.
52. Isfahani, A. P.; Ghalei, B.; Wakimoto, K.; Bagheri, R.; Sivaniah, E.; Sadeghi, M., Plasticization resistant crosslinked polyurethane gas separation membranes. *Journal of Materials Chemistry A* **2016,** 4, (44), 17431-17439.
53. Hou, J.; Li, X.; Guo, R.; Zhang, J.; Wang, Z., Mixed matrix membranes with fast and selective transport pathways for efficient CO_2 separation. *Nanotechnology* **2018,** 29, (12), 125706.

TOC

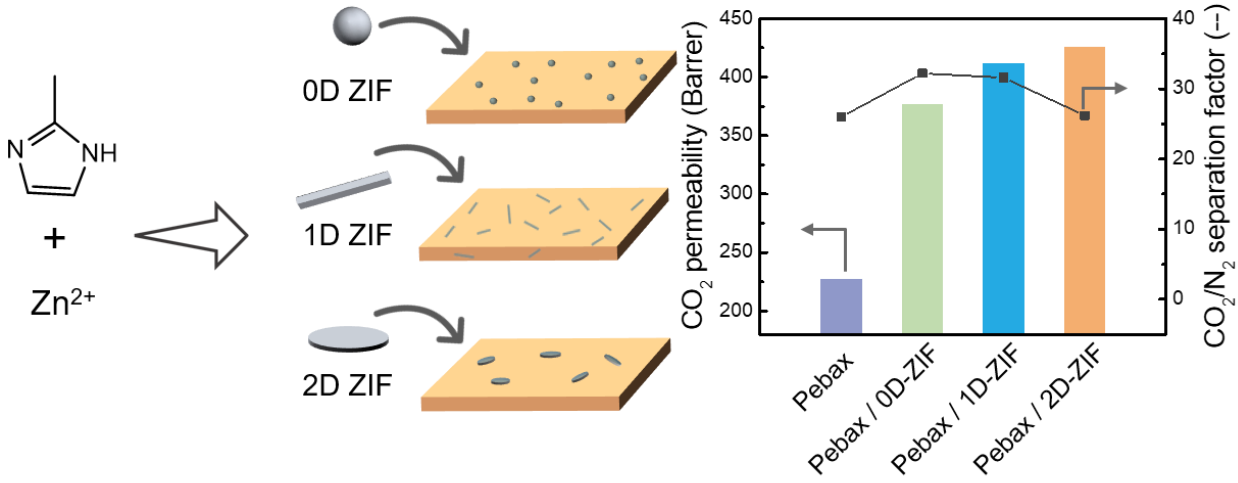
N
NH
+
Zn2+
0D ZIF
1D ZIF
2D ZIF
CO2 permeability (Barrer)
CO2/N2 separation factor (--)
450
400
350
300
250
200
40
30
20
10
0
Pebax
Pebax / 0D-ZIF
Pebax / 1D-ZIF
Pebax / 2D-ZIF